Supporting Information

Synthesis, spectroscopic and biological studies of a fluorescent Pt(II) (terpy) based 1,8-naphthalimide conjugate as a DNA targeting agent

Swagata Banerjee,[a] Jonathan A. Kitchen,[a,c] Sandra A. Bright,[b] John E. O'Brien,[a] D. Clive Williams,*[b] John M. Kelly*[a] and Thorfinnur Gunnlaugsson*[a]

General Experimental Details

All NMR spectra were recorded using either a Bruker DPX-400 or AV-600 spectrometer, operating at 400/600 MHz for ^{1}H NMR and 100/150 MHz for ^{13}C NMR, respectively. Chemical shifts were referenced relative to the internal solvent signals. Multiplicities are abbreviated as follows: singlet (s), doublet (d), triplet (t), double triplet (dt). Infrared (IR) spectra were recorded on a Perkin Elmer Spectrum 100 FT-IR spectrophotometer equipped with a Universal ATR sampling accessory. Electrospray mass spectra were recorded on a Micromass LCT spectrometer or a MALDI QToF Premier, running Mass Lynx NT V 3.4 on a Waters 600 controller connected to a 996 photodiode array detector using HPLC grade methanol, water or acetonitrile as carrier solvents. High resolution mass spectra were obtained by a peak matching method using leucine enkephalin (Tyr-Gly-Gly-Phe-Leu) as the reference (m/z = 556.2771). All accurate masses were quoted to ≤5 ppm. Melting points were determined using an Electrothermal IA9000 digital melting point apparatus. Elemental analysis of all compounds was carried out at the Microanalytical Laboratory, School of Chemistry and Chemical Biology, University of Dublin. UV/vis absorption spectra were recorded on a Varian CARY 50 spectrophotometer. All the spectroscopic measurements were carried out in quartz cuvettes (10 mm × 10 mm). The wavelength range was 200-800 nm with a scan rate of 600 nm/min. MilliQ water was used in DNA related work. Phosphate buffer: two 1 M stock solutions of Na_2HPO_4 and NaH_2PO_4 were made up with MilliQ water. Portions of each solution were diluted together to achieve 10 mM phosphate buffer of pH 7.0, which was then filtered using a 0.45 μM syringe filter. Baseline corrections were performed for all spectral measurements. All solutions were prepared fresh prior to measurement. The UV/vis titrations were carried out by monitoring the changes in the absorption spectra of the ligand of interest in 10 mM phosphate buffer (pH 7.0) upon gradual addition of mononucleotides/*st*-DNA/polynucleotides. All the titrations were repeated at least three times to ensure

reproducibility. Steady-state fluorescence spectra were recorded on a Varian Cary Eclipse spectrofluorimeter. Fluorescence titrations were carried out using optically dilute solutions (absorbance < 0.1) following the same procedure as described for UV/vis titrations. CD spectra were recorded on a JASCO J810 spectropolarimeter. Each CD trace represents the average of three scans. Linear dichroism specra were recorded on a JASCO J-815 CD spectropolarimeter equipped with a Dioptica Scientific Ltd. linear dichroism accessory. The LD spectra were presented as the average of there scans. Thermal denaturation experiments were conducted on a Perkin-Elmer35 UV/vis spectrophotometer coupled to a Peltier temperature controller. The temperature was ramped from 30°C-90°C at a rate of 1°C/min rate and the absorbance at 260 nm was measured at every 0.2°C interval. All the solutions were thoroughly degassed prior to measurement. X-ray data (ESI tables 3 and 4) were collected on either a Rigaku Saturn 724 CCD Diffractometer (for **2**) using graphite-monochromated Mo-Kα radiation (λ = 0.71073 Å) or a Bruker Apex2 Duo (for **1**) using a high intensity Cu-Kα radiation source (λ = 1.54178 Å). The data set from the Rigaku Saturn-724 diffractometer was collected using Crystalclear-SM 1.4.0 software. Data integration, reduction and correction for absorption and polarisation effects were all performed using the Crystalclear-SM 1.4.0 software. Space group determination, was obtained using Crystalstructure ver.3.8 software. The dataset collected on the Bruker Apex2 Duo was processed using Bruker APEXv2011.8-0 software. Both structures were solved by direct methods (SHELXS-97) and refined against all F^2 data (SHELXL-97).[1,2] All H-atoms were positioned geometrically and refined using a riding model with d(CH_{aro}) =0.95 Å, U_{iso} = 1.2U_{eq} (C) for aromatic, 0.99 Å, U_{iso} = 1.2U_{eq} (C) for CH_2 and 0.98 Å, U_{iso} = 1.2U_{eq} (C) for CH_3. The SQUEEZE routine of PLATON[2] was used to remove a severely disordered CH_3CN molecule of solvation (82 $Å^3$ and 24 electrons per cell).

Cell culture: HeLa (human cervical cancer) and MCF-7 (human breast cancer) cells were grown in Dulbecco's Modified Eagle Medium (Glutamax) supplemented with 10% fetal bovine serum and 50 µg/ml penicillin/streptomycin at 37˚C in a humidified atmosphere of 5% CO_2.

Alamar blue viability assay: HeLa cells were seeded at a density of $5*10^3$ cells/well and MCF-7 cells at a density of $1*10^4$ cells/well in 96-well plates and treated with the indicated compounds for 48h. Alamar blue (20µl) was then added to each well and incubated at 37°C in the dark for 4h. Plates were then read on a fluorescence plate reader (SpectraMax Gemini,

Molecular Devices) with excitement and emission wavelengths of 544nm and 590nm respectively. Experiments were performed in triplicate on three independent days with activity expressed as percentage cell viability compared to vehicle treated controls. All data points (expressed as means ± S.E.M.) were analysed using GRAPHPAD Prism (Graphpad software Inc., San Diego, CA).

Flow cytometry: HeLa cells were seeded at a density of $1*10^5$ cells/well in a 6-well plate and treated with the indicated compounds for 48h. Samples were then centrifuged at 650xg for 5 min and resuspended in 100µl ice-cold PBS. Ice-cold 70% (v/v) ethanol (1ml) was then added to fix the samples overnight at 4°C. Samples were subsequently centrifuged at 800xg for 10 min; and resuspended in 200µl phosphate buffered saline. RNase A (12.5µl of 10mg/ml) and propidium iodide (37.5µl of 1mg/ml) were and samples were incubated for 30 min at 37°C. Cell cycle analysis was performed at 488nm using a Becton Dickinson FACS Calibur flow cytometer. The Macintosh-based application CellQuest was then used to analyse the data of 10,000 gated cells once cell debris had been excluded. Data points represent the mean ± S.E.M. of two independent experiments.

Confocal microscopy: HeLa cells were seeded at a density of $1*10^5$ cells/well in glass bottom wells and treated with the indicated compounds for up to 48 hrs. Cells were washed followed by the addition of fresh media and DRAQ5 (red nuclear stain), followed by viewing using Olympus FV1000 confocal microscopy with a 60X oil immersion lens. Image analysis was performed using FluoView Version 7.1 Software. Compounds were excited by a 408nm argon laser, emission ~500nm, DRAQ5 was excited by a 633nm red helium-neon laser, emission >650nm.

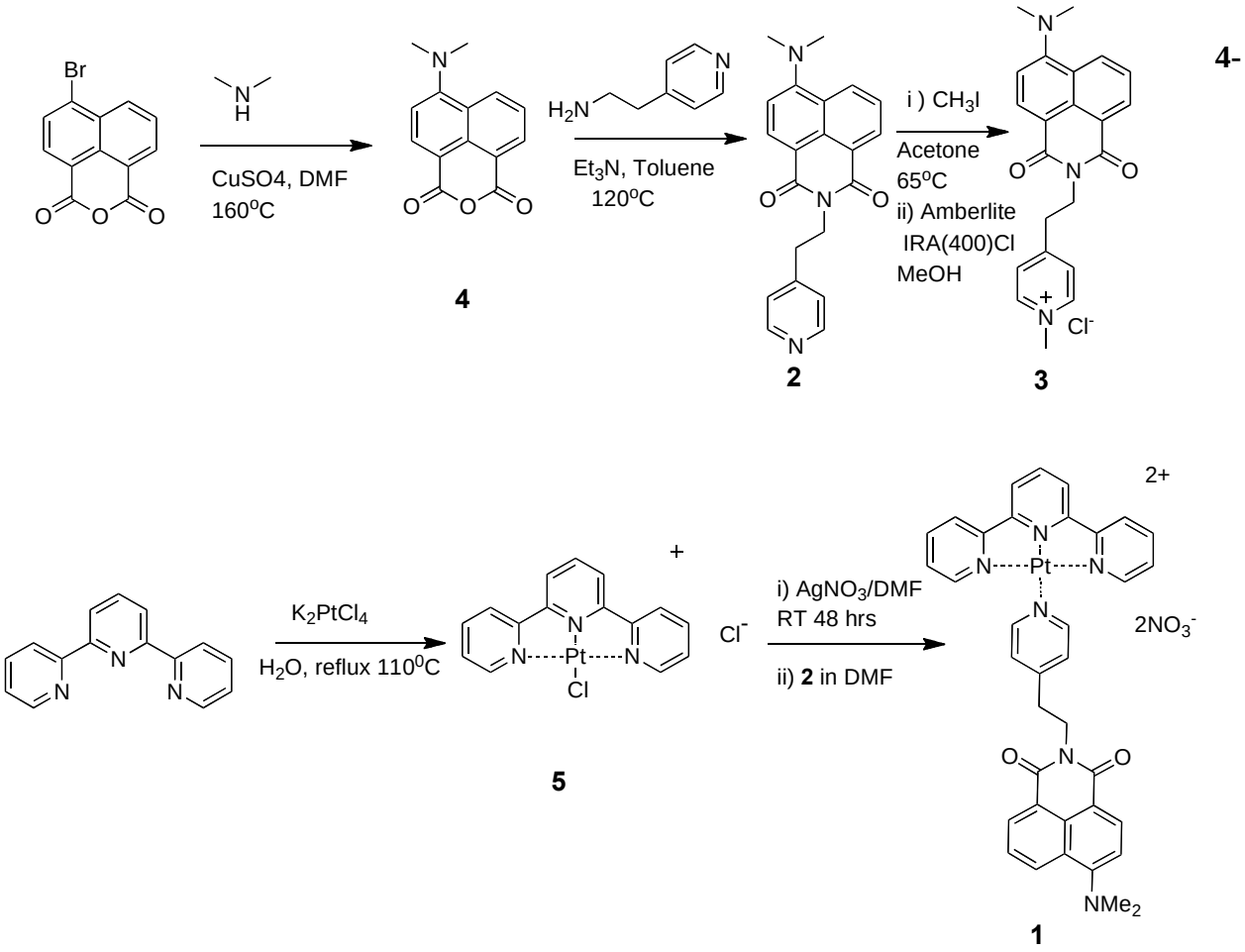

ESI Scheme 1: Synthetic scheme for **1**.

N,N' Dimethylamino-1,8-naphthalimide (4)[3]

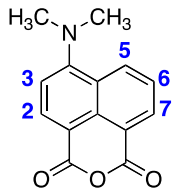

Dimethylamine (5 mL, 40% aqueous solution, excess) and $CuSO_4 \cdot 5H_2O$ (0.12 g, 0.48 mmol) were added to a suspension of 4-bromo-1,8-naphthalic anhydride (2.5 g, 9.00 mmol) in DMF (30 mL). The reaction mixture was stirred under reflux condition for 12 hrs under argon atmosphere. The solvent was removed under reduced pressure and the resulting yellow solid was purified by recrystallisation from hot methanol to yield the desired product as a bright yellow solid in 78% yield (1.70 g). m.p. (203-204)°C (Ref.3, 206°C); Found: C, 68.63; H, 4.38; N, 5.89%. $C_{14}H_{11}NO_3 \cdot 0.2 \cdot H_2O$ requires C, 68.68; H, 4.69; N, 5.72%; HRMS: Found 242.0829 ($[M + H]^+$, $C_{14}H_{12}NO_3$ requires 242.0817; δ_H (400 MHz, $CDCl_3$): 8.54 (1H, d, *J* = 8.0 Hz, Ar-H7), 8.50 (1H, d, *J* = 8.0 Hz, Ar-H5), 8.42 (1H, d, *J* = 8.0 Hz, Ar-H2), 7.68 (1H, t, *J* = 8.0 Hz,

Ar-H6), 7.10 (1H, d, *J* = 8.0 Hz, Ar-H3), 3.21 (s, 6H, $N(CH_3)_2$). δ_C (100 MHz), 161.7 (C=O), 160.7 (C=O), 157.9 (C), 134.9 (CH), 133.1 (CH), 132.9 (CH), 132.8 (C), 124.9 (CH), 124.7 (C), 119.1 (C), 113.1 (CH), 109.2 (C), 44.6 (CH_3). ν_{max} (neat sample)/ cm^{-1}: 1753, 1720, 1582, 1568, 1522, 1495, 1393, 1339, 1307, 1186, 1117, 997, 927, 774, 747

Figure ESI 1: ^1H NMR of **4** ($CDCl_3$, 400 MHz).

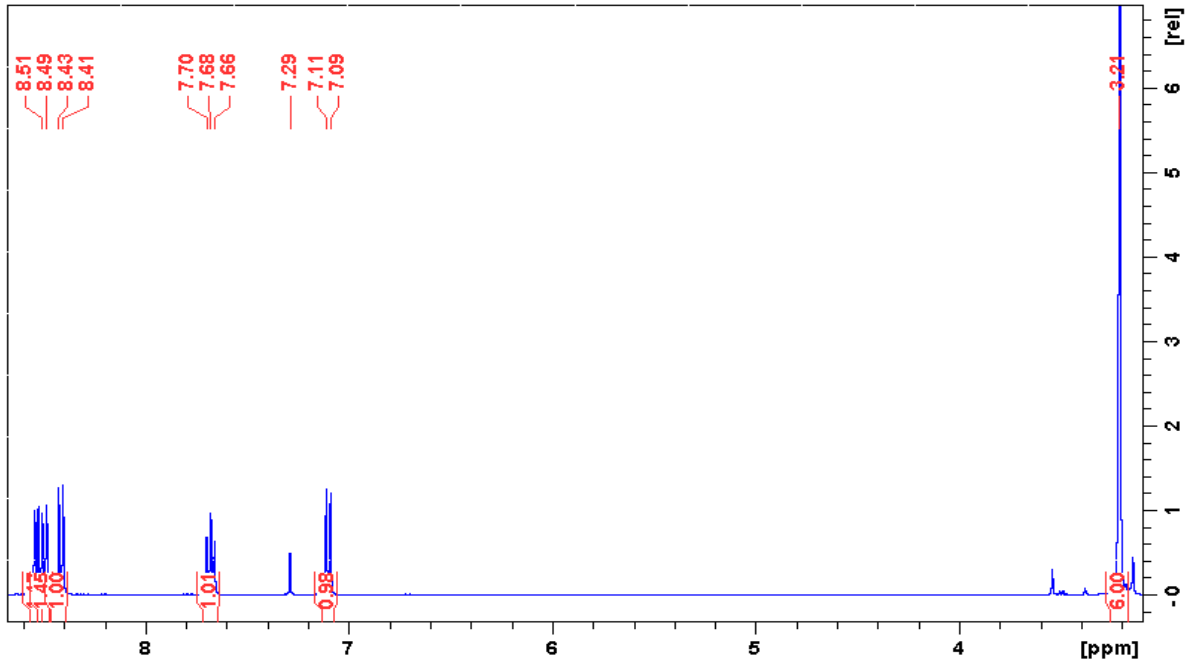

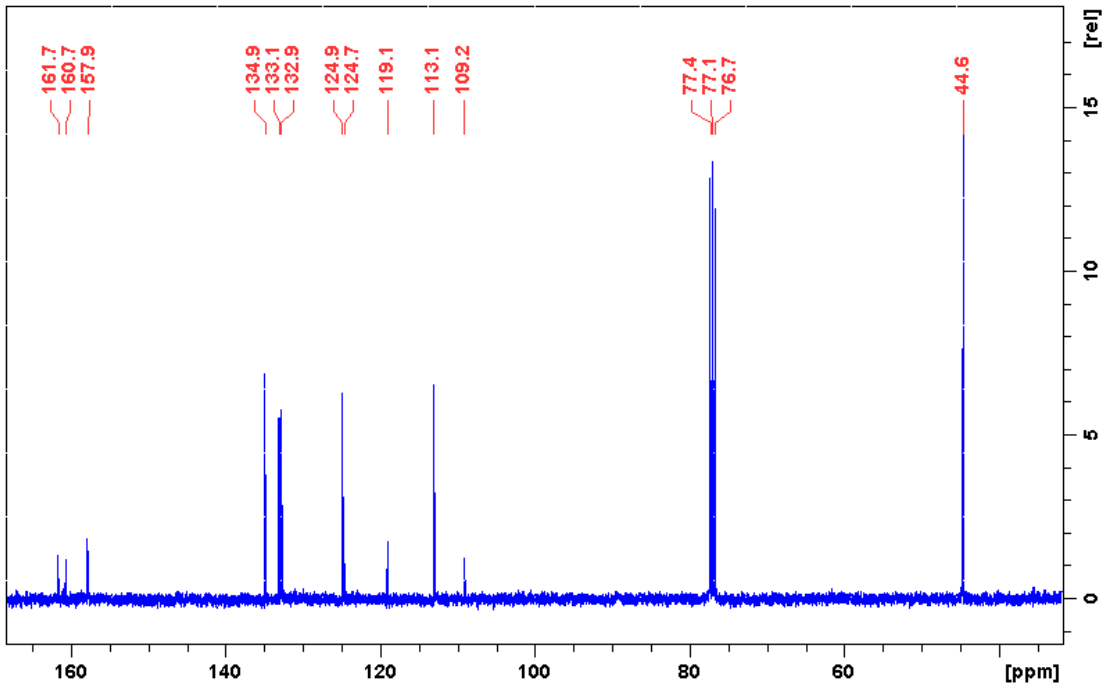

Figure ESI 2: ^{13}C NMR of **4** ($CDCl_3$, 100 MHz).

***N*-[2-(Pyridin-4-yl)ethyl]-4-*N*,*N*′-dimethylamino-1,8-naphthalimide (2)**

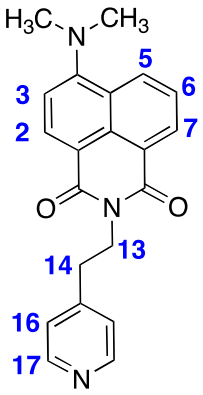

4-(2-Aminoethyl)pyridine (0.70 mL, 5.87 mmol) and triethylemine (1.20 mL, 8.80 mmol) were added to the suspension of **4** (1.03g, 4.27 mmol) in anhydrous toluene and the mixture was stirred under reflux for 3 days under an argon atmosphere. The resulting mixture was filtered through celite while still hot and washed with toluene. The solvent was removed under reduced pressure and the resultant solid was dissolved in CH_2Cl_2, washed once with saturated solution of $NaHCO_3$, followed by washing with water and brine, respectively. The organic layer was dried over $MgSO_4$ and the solvent was removed under reduced pressure. The resulting solid was purified by recrystallisation from hot methanol to yield the product as a bright yellow solid in 56% yield (0.83 g). m.p. (157.5-158)°C; Found: C, 72.79; H, 5.43; N, 12.09%. $C_{21}H_{19}N_3O_2 \cdot 0.1 \cdot H_2O$ requires C, 72.65; H, 5.57; N, 12.10%; HRMS: Found 346.1551 ($[M + H]^+$, $C_{21}H_{20}N_3O_2$ requires 346.1551). δ_H (400 MHz, $CDCl_3$), 8.57 (1H, d, J = 8.0 Hz, Ar-H7), 8.53(2H, d, J = 4.0 Hz, Py-H16), 8.48 (1H, d, J = 8.0 Hz, Ar-H2), 8.46 (1H, d, J = 8.0 Hz, Ar-H5), 7.68 (1H, t, J = 8.0 Hz, Ar-H6), 7.31 (2H, d, J = 4.0 Hz, Py-H17), 7.13 (1H, t, J = 8 Hz, Ar-H3), 4.43 (2H, t, J = 8 Hz, CH_2), 3.14 (s, 6H,

$N(CH_3)_2$), 3.06 (2H, t, J = 8 Hz, CH_2). δ_C (100 MHz): 164.5 (C=O), 163.9 (C=O), 157.2 (C), 149.6 (CH), 148.2 (C), 132.8 (CH), 131.4 (CH), 131.1 (CH), 130.3 (C). 125.3 (C), 124.9 (CH), 124.5 (CH), 122.8 (C), 114.5 (C), 113.3 (CH), 44.8 (CH3), 40.3 (CH_2), 33.6 (CH_2). ν_{max} (neat sample)/ cm^{-1}: 2965, 2843,1685, 1645, 1583, 1569, 1560, 1415, 1383, 1349, 1267, 1241, 1022, 838, 756.

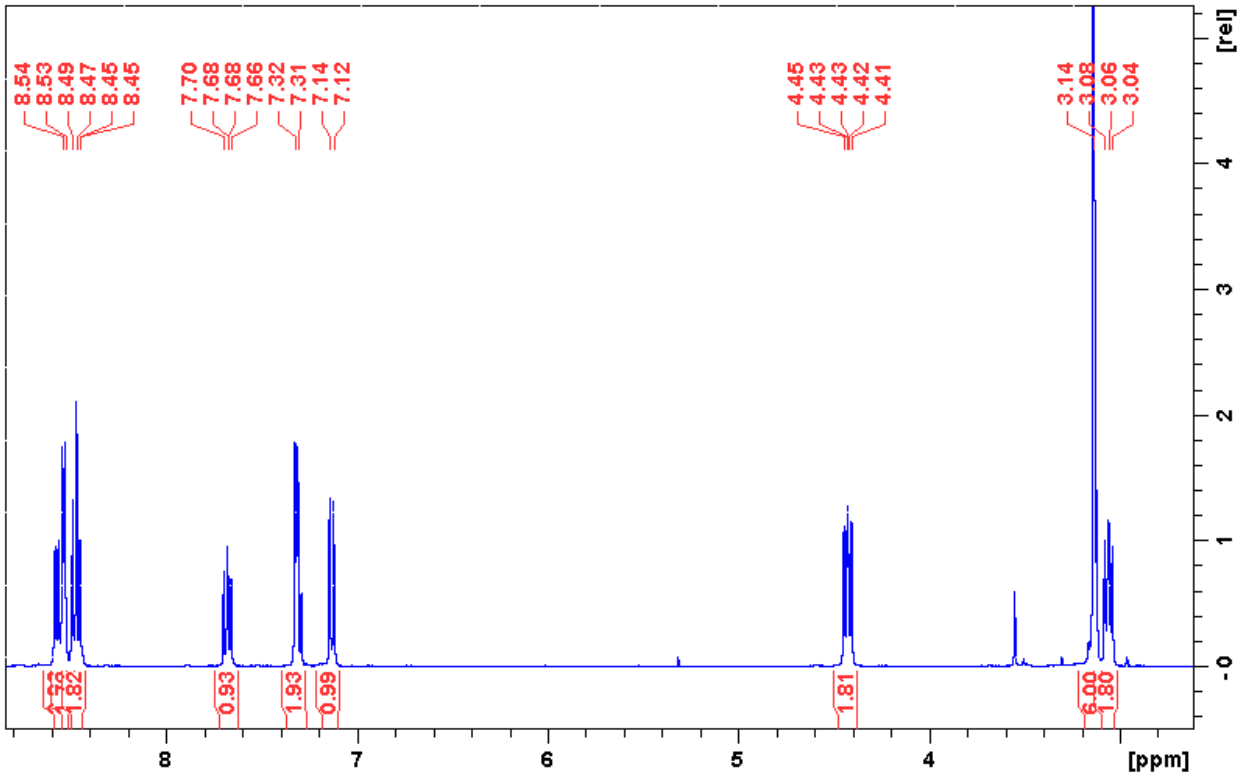

Figure ESI 3: ^{1}H NMR of **2** ($CDCl_3$, 400 MHz).

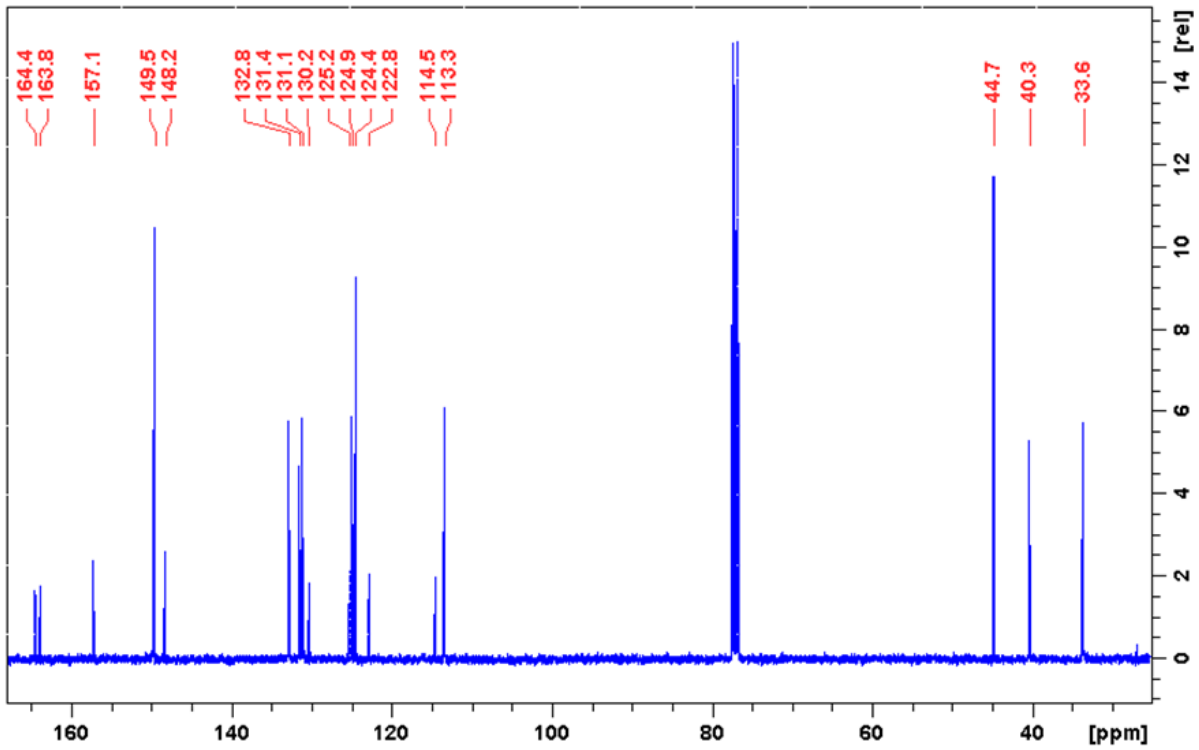

Figure ESI 4: ^{13}C NMR of **2** ($CDCl_3$, 100 MHz).

(2,2':6',2''-Terpyridine)platinum(II) chloride complex (5)[4]

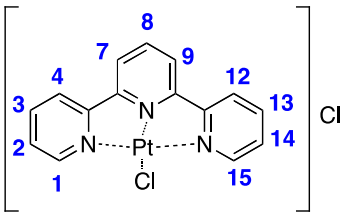

Potassium tetrachloroplatinate (K_2PtCl_4) (0.93 g, 2.24 mmol) was dissolved in minimum volume of water. To this 1 ml of dimethyl sulfoxide (DMSO) was added followed by the addition of 2,2',6',2''-terpyridine (0.52 g, 2.24 mmol) and heated under refluxing condition at 110°C till the solution became clear. The solution was cooled to room temperature and acidified using concentrated HCl. The desired product was obtained as an orange-red precipitate in 89% yield (1 g). m.p. > 300°C; HRMS: Found 463.0292 ($[M]^+$, $C_{15}H_{11}N_3ClPt$ requires 463.0289); δ_H (600 MHz, D_2O), 8.01 (1H, t, J = 8.0 Hz, Ar-H8), 7.98 (2H, t, J = 8.0 Hz, Ar-H3, Ar-H13), 7.75 (2H, d, J = 8.0 Hz, Ar-H4, Ar-H12), 7.75 (2H, d, J = 8.0 Hz, Ar-H7, Ar-H9), 7.62 (2H, d, J = 4.0 Hz, Ar-H1, Ar-H15), 7.25 (2H, t, J = 8.0 Hz, Ar-H2, Ar-H14), δ_C (150 MHz), 157.0 (C), 153.4 (C), 150.4 (CH), 142.6 (CH), 142.3 (CH), 129.1(CH), 125.3(CH), 124.1 (CH). ν_{max} (neat sample)/ cm^{-1}: 3311, 1605, 1475, 1452, 1439, 1401, 1315, 1285, 1031, 779, 722.

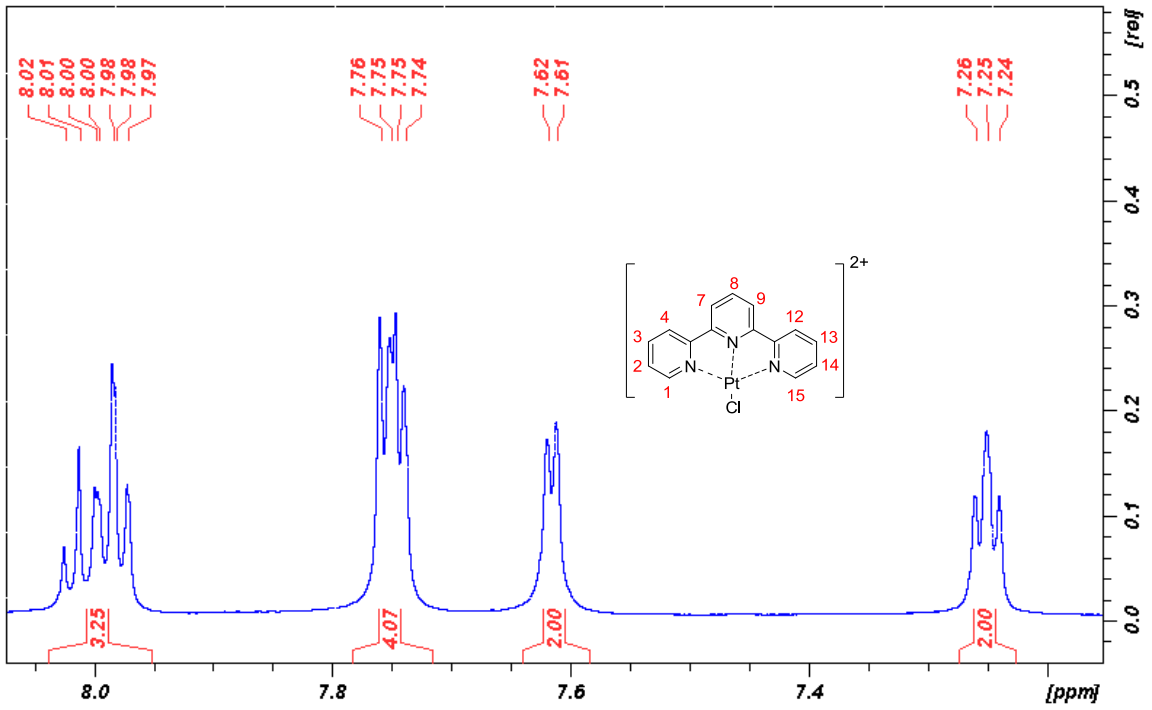

Figure ESI 5: ^{1}H NMR of **5** (D_2O, 600 MHz).

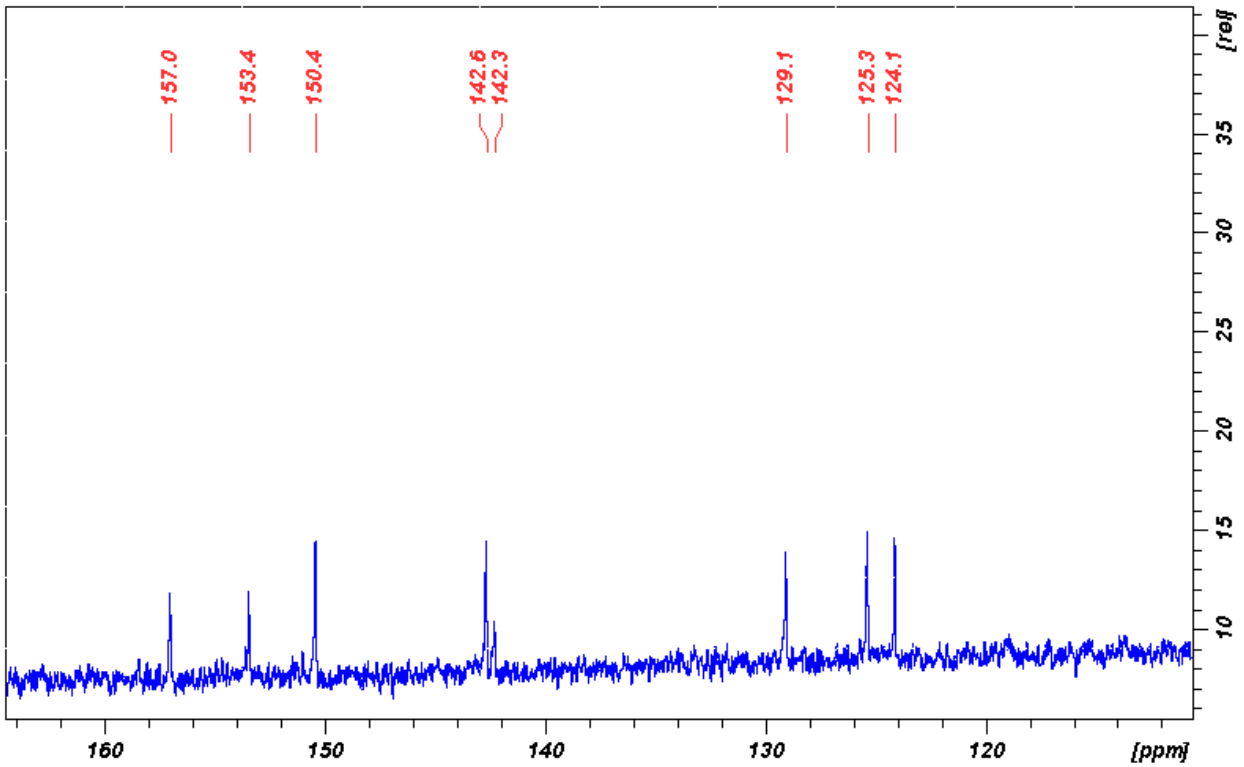

Figure ESI 6: ^{13}C NMR of **5** (D_2O, 150 MHz).

2,2':6',2''-Terpyridine(*N*-[2-(pyridin-4-yl)ethyl]-4-*N*,*N*-dimethylamino-1,8-naphthalimide)platinum(II) nitrate complex (1)

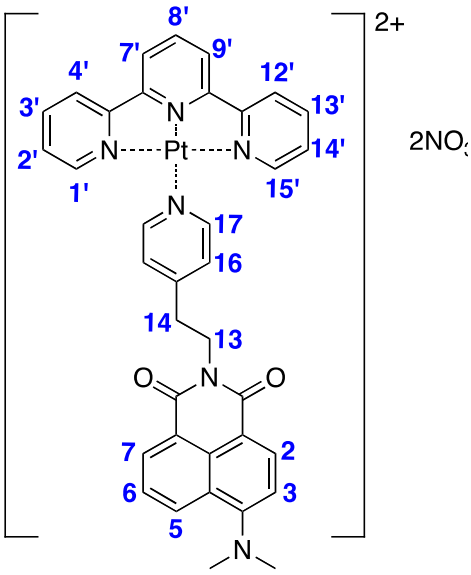

A solution of $AgNO_3$ in DMF (0.26 gm, 1.53 mmol) was added gradually to a suspension of **5** (0.40 g, 0.75 mmol) in DMF and the mixture was stirred at room temperature in the dark for 24 hrs. The resulting mixture was then filtered through celite to remove AgCl. To the resulting orange solution, a solution of **2** (0.26 gm, 0.75 mmol) in DMF was added and stirred at room temperature for 2-3 hrs. The product was precipitated from diethyl ether and obtained as a red powder after purification by trituration with methanol at room temperature in 82% yield (0.55 g). m.p. (278-279)°C; Found: C, 45.23; H, 2.97; N, 11.53%. $C_{36}H_{30}N_8O_8 \cdot 0.4 \cdot AgCl$ requires C, 45.27; H, 3.17; N, 11.73%; HRMS (ESI): Found 386.6043 (M^{2+}, $C_{36}H_{30}N_6O_2Pt$ requires 386.6039); δ_H (600 MHz, CD_3OD), 9.03 (2H, d, *J* = 6.0 Hz, Py-H17), 8.595 (1H, t, *J* = 8.0 Hz, Tpy-H8'), 8.59 (2H, d, *J* = 8.0 Hz, Tpy-H4', Tpy-H12'), 8.57 (1H, d, *J* = 8.0 Hz, Nap-H5), 8.567 (2H, t, *J* = 8 Hz, Tpy-H2', Tpy-H14'), 8.56 (2H, d, *J* = 8.0 Hz, Tpy-H7', Tpy-H9'), 8.518 (1H, d, *J* = 8.0 Hz, Nap-H7), 8.505 (2H, t, *J* = 8.0 Hz, Tpy-H3', Tpy-H13'), 8.41 (1H, d, *J* = 8 Hz, Nap-H2), 7.869 (2H, d, *J* = 4.0 Hz, Tpy-H1', Tpy-H15'), 7.866 (2H, d, *J* = 6.0 Hz, Py-H16), 7.72 (1H, t, *J* = 8.0 Hz, Nap-H6), 7.21 (1H, d, *J* = 8.0 Hz, Nap-H3), 4.57 (2H, t, *J* = 7.0 Hz, CH_2), 3.36 (2H, t, *J* = 7.0 Hz, CH_2), 3.14 (6H, s, $N(CH_3)_2$), δ_C (150 MHz), 165.1 (C=O), 164.6 (C=O), 158.9 (C), 158.2 (C), 156.6 (C),155.9 (C), 152.1 (CH), 151.6 (CH), 143.9 (CH), 143.5 (CH), 133.1 (CH), 132.5 (CH), 131.3 (CH), 130.7 (C), 129.3 (CH), 126.2 (CH), 125.3 (C), 124.9 (CH), 124.4 (CH), 122.7 (C), 113.6 (C), 113.3 (CH), 44.0 (CH_2), 40.3 (CH_2), 34.1 ($N(CH_3)_2$). ν_{max} (neat sample)/ cm^{-1}: 3075, 1683, 1640, 1566, 1450, 1328, 1251, 827, 781.

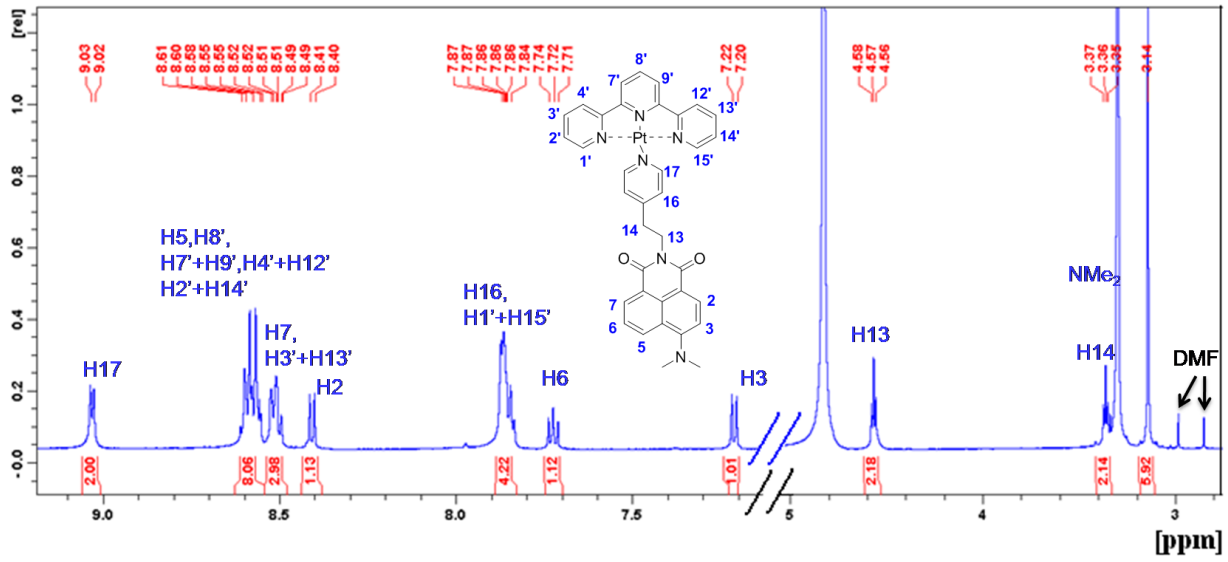

Figure ESI 7: ^{1}H NMR of **1** (CD_3OD, 600 MHz).

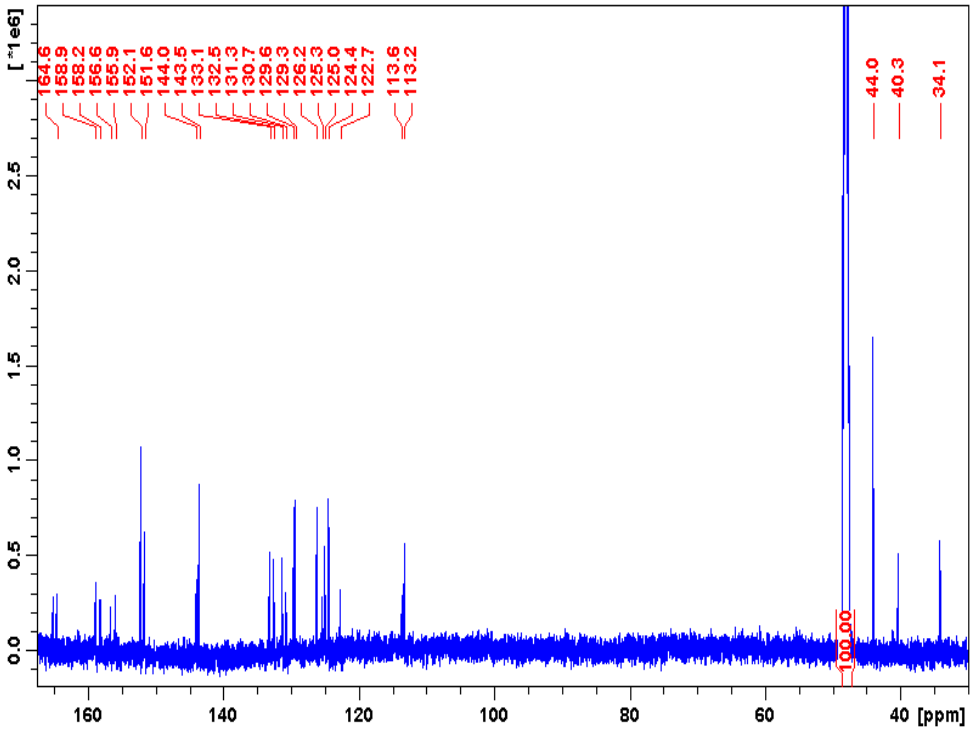

Figure ESI 8: ^{13}C NMR of **1** (CD_3OD, 150 MHz).

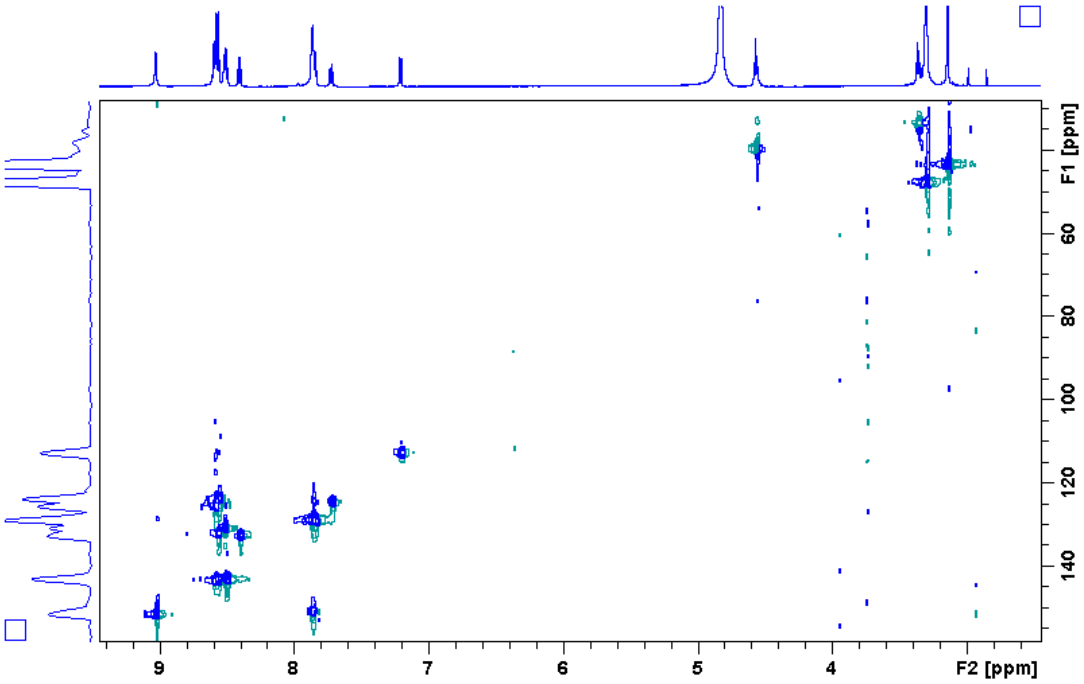

Figure ESI 9: HSQC NMR spectrum of **1** (CD_3OD, 600/150 MHz).

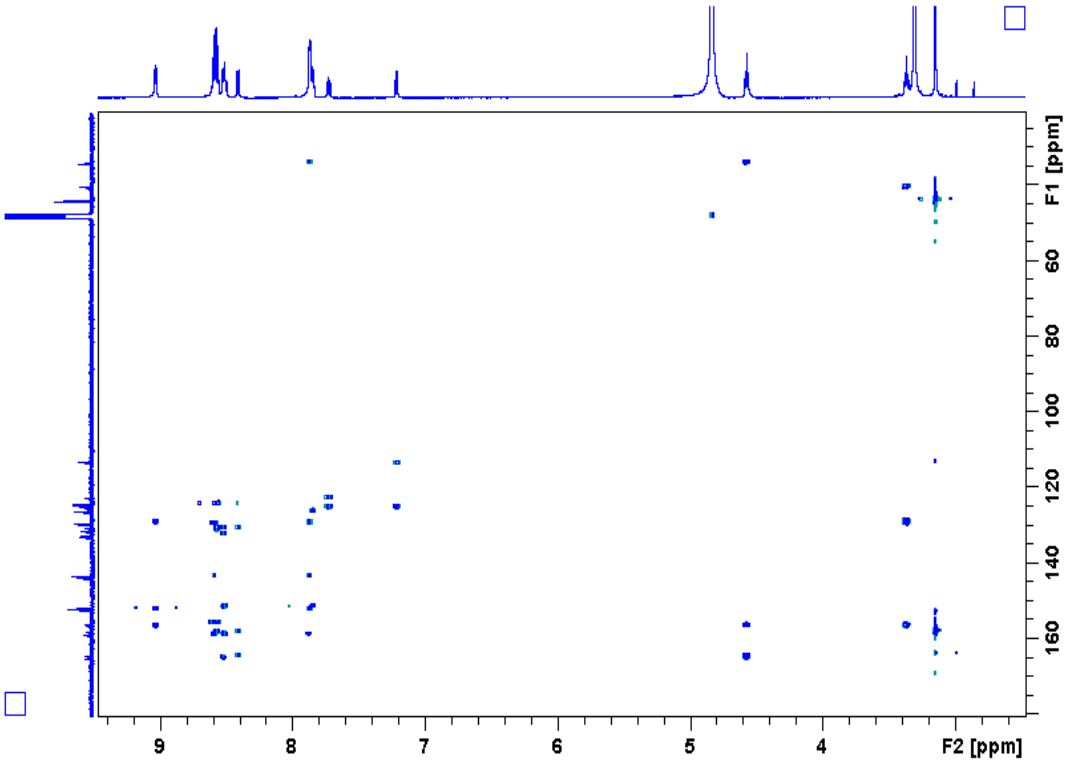

Figure ESI 10: HMBC NMR spectrum of **1** (CD_3OD, 600/150 MHz).

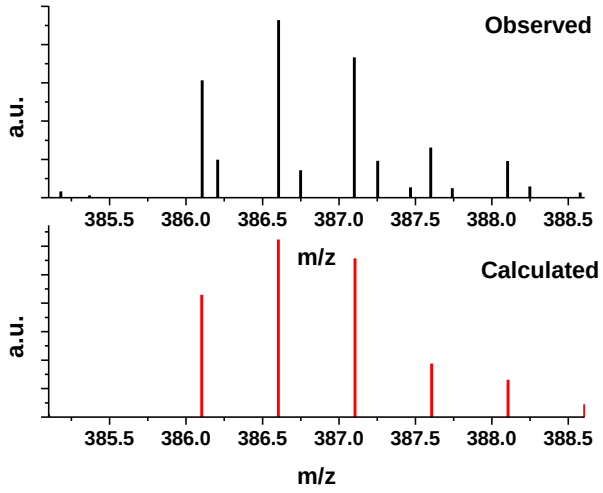

Figure ESI 11 Comparison of the calculated (bottom panel) and the observed isotopic distribution pattern for **1** from (ESI positive).

X-ray description of 2.

Small plate shaped yellow coloured crystals of 2 were grown by the slow evaporation of ethanol. The low temperature (118 K) crystal structure showed that **2** crystallised in the monoclinic space group P2(1)/n with one molecule of **2** in the asymmetric unit (Figure ESI 12a). In the solid state the ethylene linker in 2 assumes an *anti*-conformation placing the pyridyl and the naphthalimide rings in almost coplanar orientation and the NMe_2 moiety was slightly twisted out of the naphthalimide plane and the nitrogen atom adopts a tetrahedral like geometry. The packing is governed by off-set face-to-face π…π interactions between the adjacent naphtahlimide rings, resulting in a head-to-tail arrangement of the molecules with the average distances between the mean planes ranging from 3.3Å-3.4 Å (Figure ESI 12b).

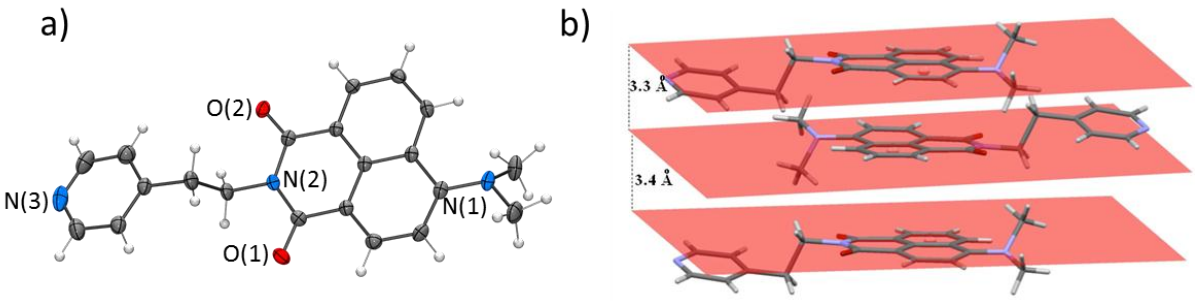

Figure ESI 12: a) The X-ray crystal structures of **2** with thermal ellipsoids shown at 50% probability. b) The packing of **2** showing the π…π interactions between the stacked naphthalimide rings which adopt a 'head-to-tail' type orientation, naphthalimide mean planes are shown as red sheets.

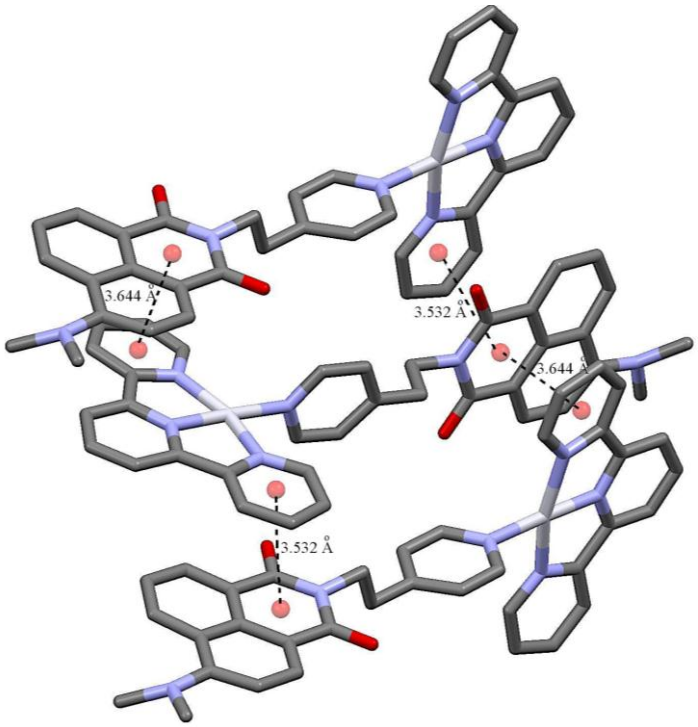

Figure ESI 13: The packing of **1** showing the π–π interactions between the stacked naphthalimide and terpyridine rings.

ESI Table 1: Selected bond lengths [Å] and angles [°] for **1.**

Bond lengths/ angles	
Pt(1)-N(5)	1.945(7)
Pt(1)-N(4)	2.028(5)
Pt(1)-N(3)	2.034(7)
Pt(1)-N(6)	2.035(6)
N(5)-Pt(1)-N(4)	81.4(2)
N(5)-Pt(1)-N(3)	177.9(2)
N(4)-Pt(1)-N(3)	97.5(2)
N(5)-Pt(1)-N(6)	81.1(2)
N(4)-Pt(1)-N(6)	162.5(2)
N(3)-Pt(1)-N(6)	99.9(2)

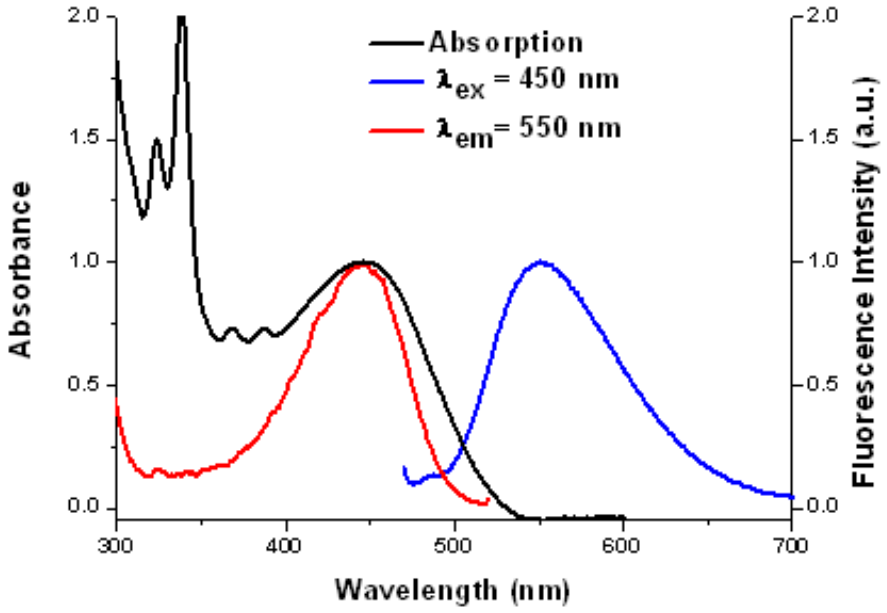

ESI Figure 14: UV/vis absorption (—), Emission (—) with λ_{ex} = 450 nm and excitation (—) spectra with λ_{em} = 550 nm of **1** in water.

.

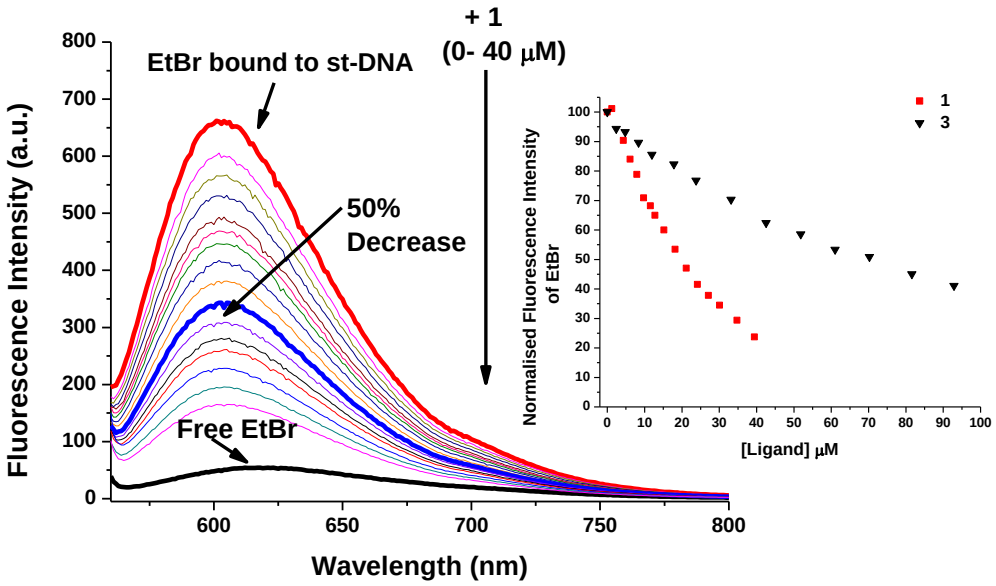

ESI Figure 15: Changes in the fluorescence spectrum of EtBr (4.75 μM) bound to *st*-DNA (9.5 μM) st-DNA in the presence of increasing concentration of **1** in 10 mM phosphate buffer. Inset: Normalised fluorescence intensity of EtBr at 600 nm upon addition of **1** and **3**.

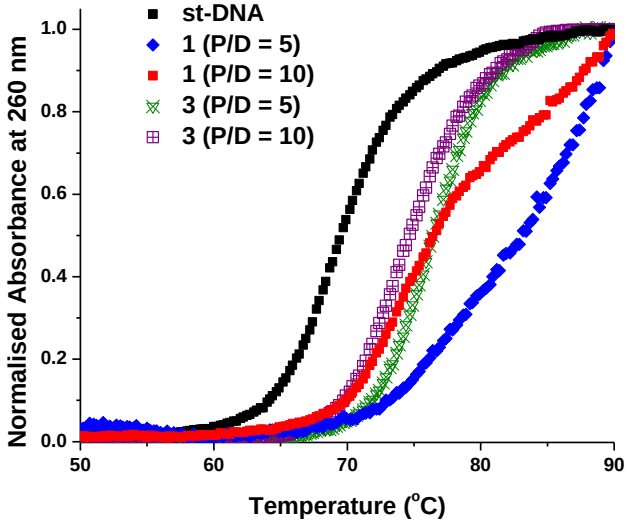

ESI Figure 16: Thermal denaturation profile of *st*-DNA (150 μM) in 10 mM phosphate buffer (pH 7.0) in the in the absence and presence of **1** and **3** at varying P/D ratios.

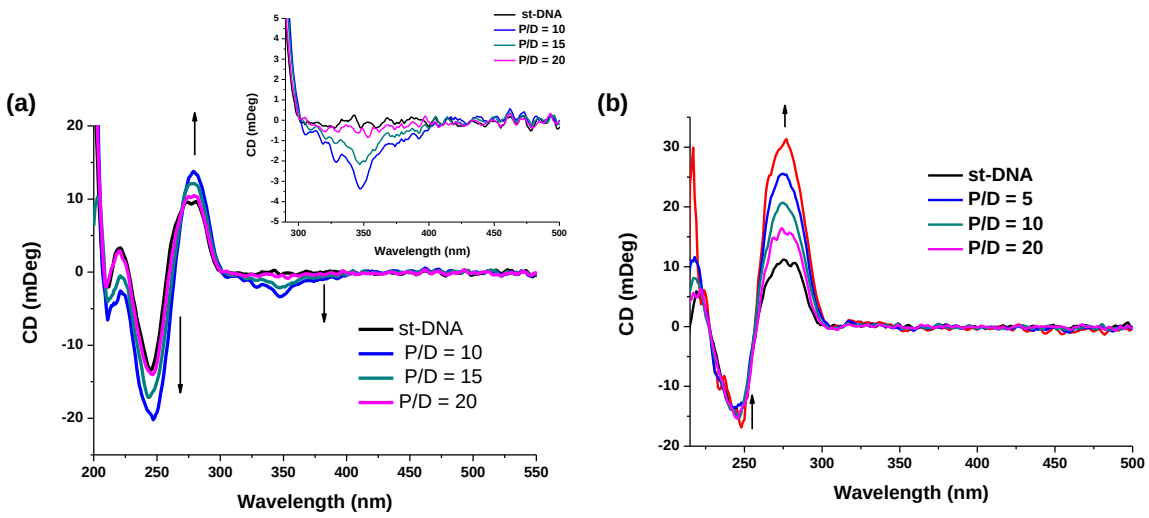

ESI Figure 17: The CD spectra of *st*-DNA (150 μM) in 10 mM phosphate buffer (pH 7.0) in the absence and presence of (a) **1** and (b) **3** at varying P/D ratios, Inset of a: ICD band in the spectral region 300-400 nm in the presence of increasing concentrations of **1**.

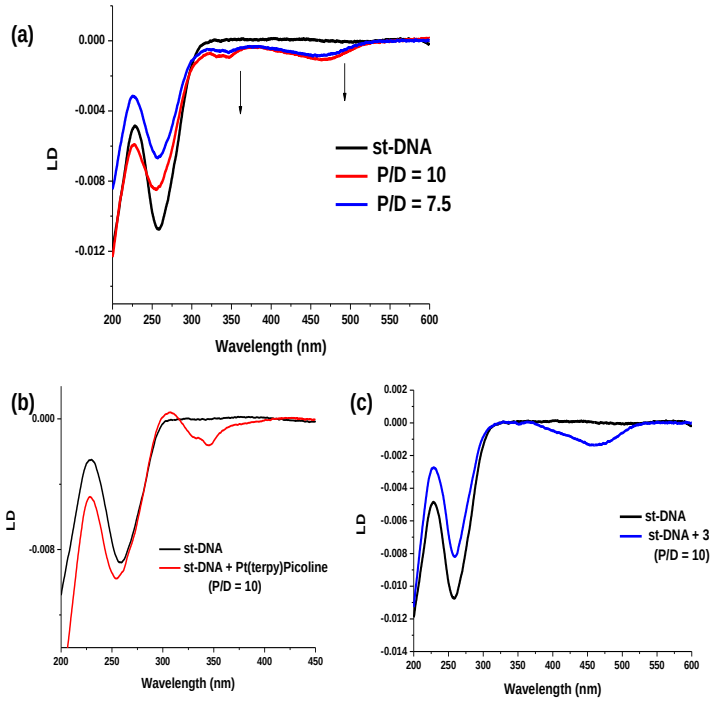

ESI Figure 18: The LD spectra of *st*-DNA (400 μM) in 10 mM phosphate buffer (pH 7.0) in the absence and presence of (a) **1,** (b) $[Pt(terpy)picoline]^{2+}$and (c) **3** at varying P/D ratios.

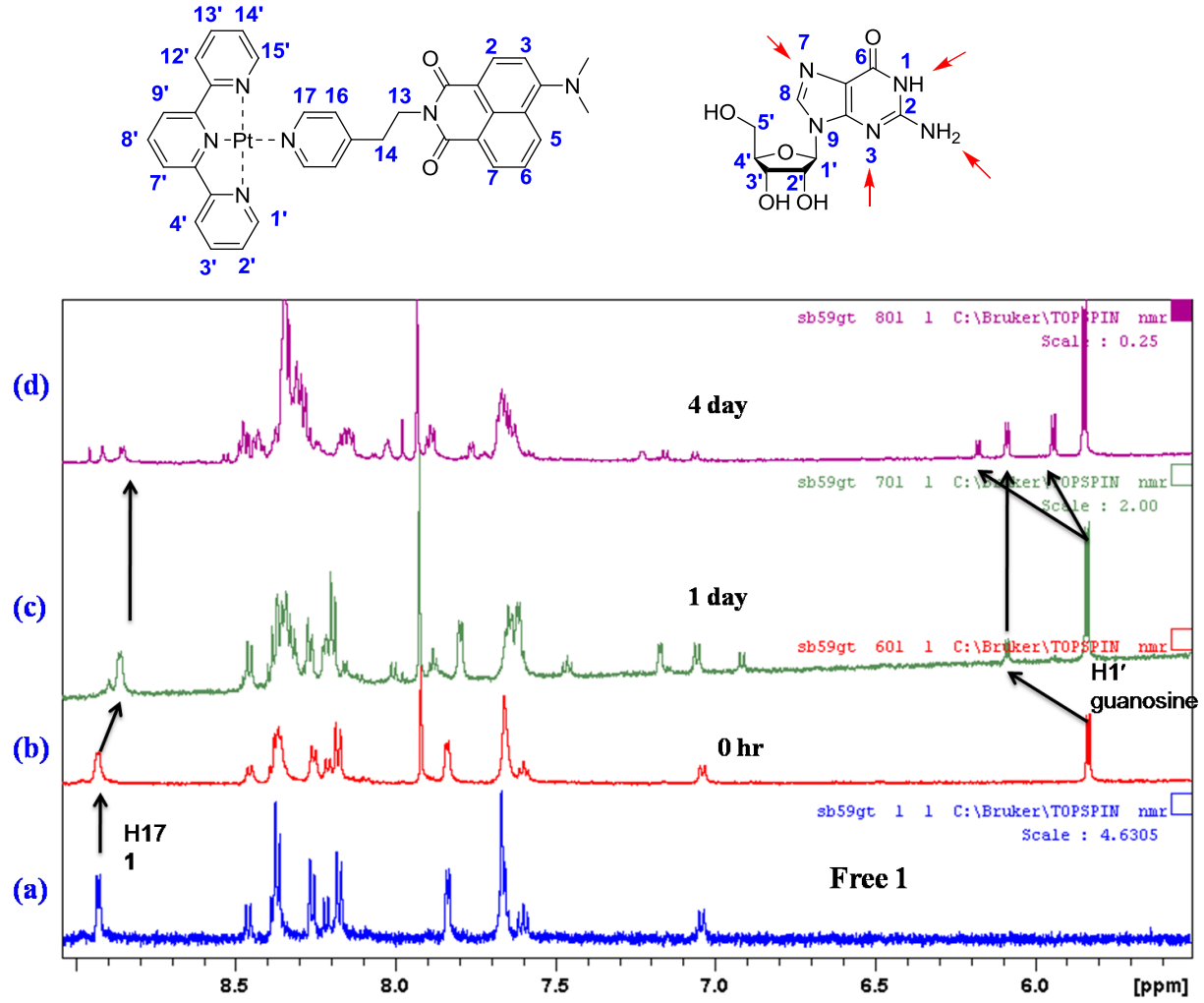

ESI Figure 19: Top panel represents the structure and numbering of **1** and guanosine and the bottom panel represents the ^{1}H NMR spectra of (a) **1** (0.5 mM), (b) **1** (0.5 mM) in the presence of guanosine (0.75 mM) immediately after addition, (c) ^{1}H NMR spectrum of the mixture after 1 day and (d) ^{1}H NMR spectrum of the mixture after 4 days in D_2O (600 MHz).

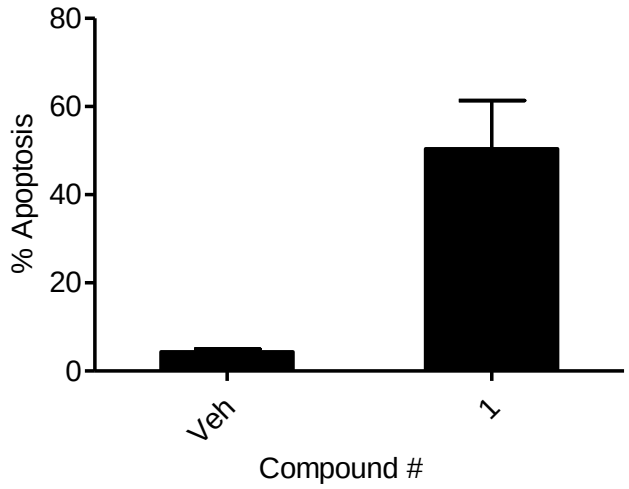

ESI Figure 20: HeLa cells were treated for 48h with a vehicle (Veh) or compound **1** (50µM). After the required incubation period, cells were fixed in 1ml ethanol and 100µl PBS and stained with propidium iodide. Cells were subsequently analysed by flow cytometry, the percentage of apoptosis was assessed by quantification of the pre-G1 peak. Values represent the mean ± S.E.M. of two independent experiments.

ESI Table 2: Summary of the IC_{50} values obtained from alamar blue assay.

Compound #	MCF-7 cells: EC50 value (**µM**)	HeLa cells: EC50 value (**µM**)
cis-platin	8.83	12.2
[Pt(terpy)Cl]Cl	>100	>100
$[Pt(terpy)(4\text{-picoline})]^{2+}$	>100	>100
1	16.6	40.7
2	50	33.6
3	>100	>100

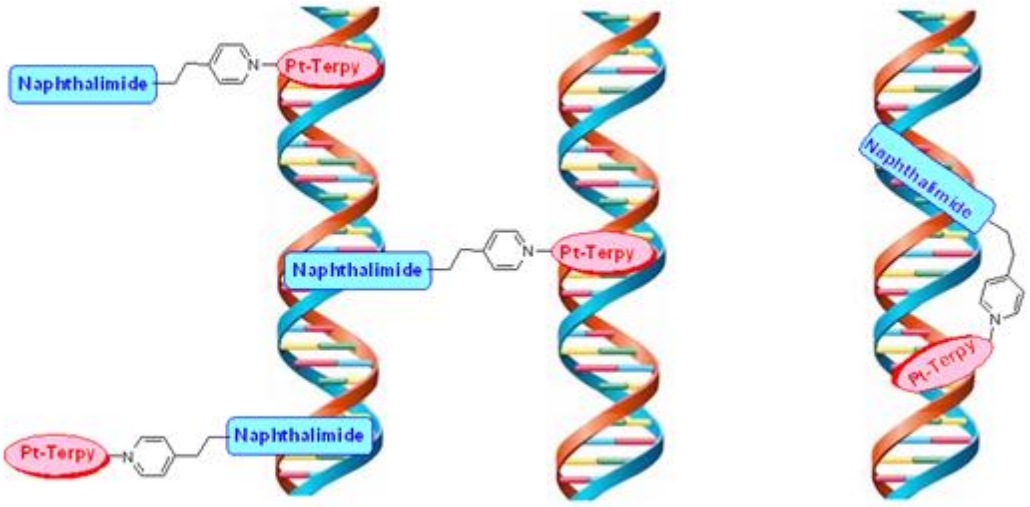

ESI Figure 21: Possible mode of binding of compound 1 to DNA.

ESI Table 3: Crystal data and structure refinement for **1**.

CCDC identification code	939038	
Identification code	sb59_4-sr	
Empirical formula	C_{38} H_{33} N_9 O_8 Pt	
Formula weight	938.82	
Temperature	100(2) K	
Wavelength	1.54178 Å	
Crystal system	Monoclinic	
Space group	C2/c	
Unit cell dimensions	a = 35.5267(13) Å	α= 90°.
	b = 10.0283(4) Å	β= 101.185(2)°.
	c = 21.7394(8) Å	γ = 90°.
Volume	7598.0(5) $Å^3$	
Z	8	
Density (calculated)	1.641 Mg/m^3	
Absorption coefficient	7.457 mm^{-1}	
F(000)	3728	
Crystal size	0.46 x 0.03 x 0.03 mm^3	

Theta range for data collection	2.54 to 64.50°.
Index ranges	-36<=h<=41, -11<=k<=11, -19<=l<=25
Reflections collected	14388
Independent reflections	6060 [R(int) = 0.0468]
Completeness to theta = 64.50°	94.8 %
Absorption correction	Semi-empirical from equivalents
Max. and min. transmission	0.8072 and 0.1307
Refinement method	Full-matrix least-squares on F^2
Data / restraints / parameters	6060 / 3 / 517
Goodness-of-fit on F^2	1.076
Final R indices [I>2sigma(I)]	R1 = 0.0580, wR2 = 0.1599
R indices (all data)	R1 = 0.0666, wR2 = 0.1687
Largest diff. peak and hole	2.367 and -2.317 e.Å^{-3}

ESI Table 4: Crystal data and structure refinement for **2.**

CCDC identification code	939037	
Identification code	sb58	
Empirical formula	C_{21} H_{19} N_3 O_2	
Formula weight	345.39	
Temperature	118(2) K	
Wavelength	0.71073 Å	
Crystal system	Monoclinic	
Space group	P2(1)/n	
Unit cell dimensions	a = 14.785(3) Å	α= 90°.
	b = 7.1200(14) Å	β= 108.28(3)°.
	c = 17.076(3) Å	γ = 90°.
Volume	1706.9(6) Å^3	
Z	4	
Density (calculated)	1.344 Mg/m^3	
Absorption coefficient	0.088 mm^{-1}	
F(000)	728	
Crystal size	0.60 x 0.54 x 0.18 mm^3	
Theta range for data collection	2.20 to 25.00°.	
Index ranges	-17<=h<=17, -8<=k<=6, -16<=l<=20	
Reflections collected	13930	

Independent reflections	2980 [R(int) = 0.0197]
Completeness to theta = 25.00°	99.0 %
Absorption correction	Semi-empirical from equivalents
Max. and min. transmission	1.0000 and 0.6295
Refinement method	Full-matrix least-squares on F^2
Data / restraints / parameters	2980 / 0 / 237
Goodness-of-fit on F^2	1.118
Final R indices [I>2sigma(I)]	R1 = 0.0402, wR2 = 0.1032
R indices (all data)	R1 = 0.0416, wR2 = 0.1044
Largest diff. peak and hole	0.196 and -0.160 e.Å^{-3}

References

1. G. M. Sheldrick, *Acta Crystallogr*., *Sect. A*, 2008, **A64**, 112

2. A.L.Spek, Acta Cryst. 2009, **D65**, 148-155

3. K. J. Kilpin, C. M. Clavel, F. Edafe and P. J. Dyson, *Organometallics*, 2012, **31**, 7031.

4. Y.-C. Lo, T.-P. Ko, W.-C. Su, T.-L. Su and A. H. J. Wang, *J. Inorg. Biochem.*, 2009, **103**, 1082.